

A Cu(II) Complex Targeting the Translocator Protein: *In Vitro* and *In Vivo* Antitumor Potential and Mechanistic Insights

D. Montagner, B. Fresch, K. Browne, V. Gandin* and A. Erxleben*

Supplementary Information

Experimental details

Materials and synthetic methods

2-Methylsilylthiazole was purchased from TCI Europe. 3-Methoxycarbonylpropionyl chloride, pyridinium bromide perbromide, dipropylamine, copper(II) bromide and tripropylamine were acquired from Sigma Aldrich. 2-Amino-3,5-dichloropyridine was bought from Alfa Aesar. 6-Cl-HOBt (6-chloro-1-hydroxybenzotriazole dihydrate) was purchased from Activotec and *N,N'*-diisopropylcarbodiimide was bought from Acros Organics.

All the solvents were of analytical grade and were used without further purification except for tetrahydrofuran and ethanol that were purified using an anion-exchange resin in order to remove all traces of water. Other chemicals used were anhydrous sodium sulfate (Fischer Scientific), sodium bicarbonate (Merck), sodium hydroxide and hydrochloric acid (VWR International). All reactions were performed under a nitrogen atmosphere. Solvents were evaporated under vacuum using a rotary evaporator or a high vacuum pump.

Compounds were purified by column chromatography using silica gel 60 (Sigma Aldrich, 230-400 mesh). Fractions were monitored using thin layer chromatography plates. The UV-detector used to analyse these plates was a Spectroline ENF-240C/FE operating at 254 nm.

TZ6 was synthesized according to the literature with some modifications (Fig. S2).¹ The literature procedures for **a** and **b** in Fig. S2 were followed without modifications.

Syntheses

Methyl [6,8-dichloro-2-(1,3-thiazol-2-yl)imidazo[1,2- α]pyridin-3-yl]acetate (c): b (1.14 g, 4.11 mmol) was added to a stirred solution of 2-amino-3,5-dichloropyridine (0.67 g, 4.11 mmol) in 15 mL dry ethanol. The mixture was refluxed for 48 h. NaHCO₃ (0.17 g, 2.05 mmol) was added in three portions after refluxing for 2 h, 6 h and 20 h, respectively. The mixture was cooled in a freezer for 24 h before being filtered and washed with two 15 mL aliquots of cold water. The resulting white solid was dried under high vacuum. Yield: 1.17 g (84 %). ¹H NMR (CDCl₃): δ 7.99 (d, *J* = 1.6 Hz, 1H, Ar), δ 7.89 (d, *J* = 3.2 Hz, 1H, Ar), δ 7.39 (d, *J* = 3.2 Hz, 1H, Ar), δ 7.33 (d, *J* = 1.6 Hz, 1H, Ar), δ 4.66 (s, 2H, CH₂CO), δ 3.74 (s, 3H, OCH₃); ESI-MS *m/z* 341.97 [M + H]⁺ (C₁₃H₁₀Cl₂N₃O₂S).

[6,8-Dichloro-2-(1,3-thiazol-2-yl)imidazo[1,2- α]pyridin-3-yl]acetic acid (d): c (1.43 g, 4.21 mmol) was dissolved in 40 mL *n*-butanol. 30 mL 0.4 M NaOH was added dropwise. The mixture was stirred at room temperature for 18 h. The solvent was removed under vacuum and the resulting residue was treated twice with a 300 mL aliquot of a H₂O/CHCl₃ (1:1) mixture. The aqueous phases were separated, combined and acidified to pH 4 with 0.1 M HCl until a red-brown solid precipitated which was collected by filtration and dried under vacuum. Yield 0.58 g (43 %). ¹H NMR (DMSO-*d*₆): δ 8.87 (d, *J* = 1.2 Hz, 1H, Ar), δ 7.96 (d, *J* = 3.2 Hz, 1H, Ar), δ 7.79 (d, *J* = 3.2 Hz, 1H, Ar), δ 7.75 (d, *J* = 1.2 Hz, 1H, Ar), δ 4.57 (s, 2H, CH₂CO); ESI-MS *m/z* 326.96 [M - H]⁻ (C₁₂H₆Cl₂N₃O₂S).

2-[6,8-Dichloro-2-(1,3-thiazol-2-yl)H-imidazo[1,2- α]pyridin-3-yl]-*N,N*-dipropylacetamide (TZ6): 6-Cl-HOBt (0.38 g, 1.85 mmol), *N,N'*-diisopropylcarbodiimide (350 μ L, 1.85 mmol) and dipropylamine (303 μ L, 1.85 mmol) were added to a stirred solution of **d** (0.50 g, 1.52 mmol) in anhydrous THF (40 mL). The mixture was left to stir at room temperature for 10 min and 318 μ L of triethylamine (2.3 mmol) was added dropwise. The mixture was left stirring for 24 h. The solvent was removed under vacuum and the resulting residue was purified by column chromatography on silica gel (mobile phase: petroleum ether/ethyl acetate 7:3). Yield 0.27 g (43 %). ¹H NMR (acetone-*d*₆): δ 8.54 (d, *J* = 1.6 Hz,

1H, Ar), δ 7.82 (d, J = 3.2 Hz, 1H, Ar), δ 7.56 (d, J = 3.2 Hz, 1H, Ar), δ 7.41 (d, J = 1.6 Hz, 1H, Ar), δ 4.73 (s, 2H, CH₂CO), δ 3.4 (t, J = 10 Hz, 2H, CH₂CH₂CH₃), δ 3.16 (t, J = 10 Hz, 2H, CH₂CH₂CH₃), δ 1.63 (m, J = 17.5 Hz, 2H, CH₂CH₂CH₃), δ 1.39 (m, J = 17.5 Hz, 2H, CH₂CH₂CH₃), δ 0.82 (t, J = 10 Hz, 3H, CH₂CH₂CH₃), δ 0.68 (t, J = 10 Hz, 3H, CH₂CH₂CH₃); ESI-MS m/z 411.07 [M + H]⁺ (C₁₈H₂₁Cl₂N₄OS).

[CuBr₂(TZ6)] (1): TZ6 (0.20 g, 0.49 mmol) was dissolved in 10 mL acetonitrile and 10 mL dichloromethane. CuBr₂ (0.11 g, 0.49 mmol), dissolved in 10 mL acetonitrile, was added dropwise at 40 °C and the mixture was left stirring for 24 h. The mixture was filtered and the filtrate was dried under vacuum giving **1** as a greenish-red solid. Yield 0.19 g (62 %). Elem. anal.: Calcd. for C₁₈H₂₀CuBr₂Cl₂N₄OS: C, 34.06; H, 3.18; N, 8.83; S, 5.05. Found: C, 33.72; H, 3.35; N, 8.58; S, 5.45. ESI-MS m/z : 553.91 [M - Br]⁺ (C₁₈H₂₀CuBrCl₂N₄OS, Figure S3). Small greenish-red needles suitable for X-ray analysis were obtained after slow evaporation of a solution of **1** in CH₃CN at room temperature.

Measurements

¹H-NMR spectra were recorded on a Jeol ECX-400 instrument operating at 400 MHz. Standard pulse sequences were used. Chemical shifts are in δ (ppm) and coupling constants J in Hz. ¹H chemical shifts were referenced to the residual solvent peaks of CDCl₃ (δ 7.25), DMSO-*d*₆ (δ 2.50) or acetone-*d*₆ (δ 2.05). Electrospray ionization mass spectrometry was conducted using a Waters LCT Premiere XE Mass Spectrometer with an Orthogona TOF Mass Analyser. Elemental analyses were carried out using a Perkin Elmer 2400 Series II CHNS/O Analyzer.

X-ray analysis

Crystal data for compound **1** were collected at 150 K on an Agilent (formerly OxfordDiffraction) Xcalibur CCD diffractometer using graphite-monochromated Mo-K α radiation (λ = 0.71069 Å).² The structure was solved by direct methods and subsequent Fourier syntheses and refined by full-matrix least squares on F^2 using SHELXS-97, SHELXL-2014 and Oscaleil.^{3,4} Hydrogen atoms except those attached to the carbon atoms of the disordered propyl groups were generated geometrically and refined as riding atoms with isotropic displacement factors equivalent to 1.3 times those of the atom to which they were attached. Due to the small crystal size and limited data quality, only the heavy atoms (Cu, Br, Cl) and the coordination sphere atoms were refined anisotropically in order to save parameters. Graphics were produced with ORTEP.⁵ Crystallographic data and details of refinement are reported in Table S1 and bond length, angles (°) and torsion angles (°) are reported in Table S2.

Biological studies

Experiments with cultured human cells

Complex **1** was dissolved in DMSO just before running the experiment and a calculated amount of drug solution was added to the cell growth medium to a final DMSO concentration of 0.5 %, which had no detectable effect on cell viability. Cisplatin and oxaliplatin were dissolved in 0.9 % NaCl solution. MTT (3-(4,5-dimethylthiazol-2-yl)-2,5-diphenyltetrazolium bromide), cisplatin, oxaliplatin, and DTNB were obtained from Sigma Chemical Co, St. Louis, USA.

Cell cultures

Human lung (A549), breast (MCF-7), colon (HCT-15 and LoVo), kidney (A498), ovarian (A2780) and pancreatic (BxPC3) carcinoma cell lines along with melanoma (A375) cells and human lung MRC-5 fibroblasts were obtained from American Type Culture Collection (ATCC, Rockville, MD). Human

embryonic kidney (HEK293) cells and human colon CCD-18Co fibroblasts were obtained from European Collection of Cell Cultures (ECACC, Salisbury, UK). The human ovarian cancer cell line 2008 and its cisplatin resistant variant, C13*, were kindly provided by Prof. G. Marverti (Department of Biomedical Science of Modena University, Italy). A431 are human cervical carcinoma cells kindly provided by Prof. F. Zunino (Division of Experimental Oncology B, Istituto Nazionale dei Tumori, Milan, Italy). Human colon carcinoma multidrug-resistant sub-line (LoVo MDR) was kindly provided by Prof. F. Majone (Department of Biology, University of Padova, Italy). The human colon carcinoma LoVo-OXP cells were derived, using a standard protocol, by growing LoVo cells in increasing concentrations of oxaliplatin and following 17 months of selection of resistant clones, as previously described.⁶ Cell lines were maintained in the logarithmic phase at 37 °C in a 5 % carbon dioxide atmosphere using the following culture media containing 10 % foetal calf serum (Euroclone, Milan, Italy), antibiotics (50 units/mL penicillin and 50 µg/mL streptomycin) and 2 mM L-glutamine: i) RPMI-1640 medium (Euroclone) for MCF-7, A431, BxPC3, A2780, 2008 and C13* cells; ii) F-12 HAM'S (Sigma Chemical Co.) for A549, LoVo, LoVo MDR and LoVo-OXP cells; iii) DMEM for A375 and HEK293 cells; iv) MEM (Sigma Chemical Co.) for A498, MRC-5 and CCD-18Co cells.

MTT assay

The growth inhibitory effect towards tumor cells was evaluated by means of MTT assay. Briefly, 3–8 x 10³ cells/well, dependent upon the growth characteristics of the cell line, were seeded in 96-well microplates in growth medium (100 µL). After 24 h, the medium was removed and replaced with a fresh one containing the compound to be studied at the appropriate concentration. Triplicate cultures were established for each treatment. After 72 h, each well was treated with 10 µL of a 5 mg/mL MTT saline solution, and following 5 h of incubation 100 µL of a sodium dodecylsulfate (SDS) solution in 0.01 M HCl was added. After an overnight incubation, cell growth inhibition was detected by measuring the absorbance of each well at 570 nm using a Bio-Rad 680 microplate reader. The mean absorbance for each drug dose was expressed as a percentage of the control untreated well absorbance and plotted vs. drug concentration. IC₅₀ values, the drug concentrations that reduce the mean absorbance at 570 nm to 50 % of those in the untreated control wells, were calculated by a four parameter logistic (4-PL) model. The evaluation was based on means from at least four independent experiments.

TSPO binding

The binding affinity of complex **1** for the TSPO was measured by competition experiments against [³H]PK11195 in the mitochondrial fractions of MCF-7 cells. Cells were homogenized and mitochondria-enriched fractions were obtained by the Mitochondria Isolation Kit (Sigma, USA) according to the manufacturer's instructions. Drug-displacement experiments were performed with membranes incubated in the presence of a constant radioligand concentration ([³H]PK 11195, 3 nM) and various non-labelled ligand concentrations up to 30 µM. The dissociation constants (IC₅₀) for complex **1** and TZ6 (S) were determined by curve fitting using the following equation, where Y is the bound ligand:

$$Y = \frac{100 \times (IC_{50})^{nH}}{IC_{50}^{nH} \times S^{nH}}$$

A Hill number (nH) value of 1±0.1 was obtained in all fittings. Protein levels were quantified using the BioRad assay.

TSPO quantification by ELISA tests

Human lung (A549), breast (MCF-7), colon (HCT-15), and pancreatic (BxPC3) carcinoma cells (10^6) were harvested and homogenized in PBS followed by centrifugation at 4 °C for 15 min at 13,000g. The supernatants were used to measure the concentrations of TSPO using the ELISA kits (Antibodies-online, Germany). According to the manufacturer's instructions, the absorbance was detected at 450 nm.

ROS production

The production of ROS was measured in MCF-7 cells (10^4 per well) grown for 24 h in 96-well plates in RPMI-1640 medium without phenol red (Sigma Chemical Co.). Cells were then washed with PBS and loaded with 10 μ M 5-(and-6)-chloromethyl-2',7'-dichlorodihydrofluorescein diacetate, acetyl ester (CM-H₂DCFDA, Molecular Probes-Invitrogen) for 25 min in the dark. Afterwards, the cells were washed with PBS and incubated with increasing concentrations of the tested complex. The fluorescence increase was estimated with a plate reader (Fluoroskan Ascent FL, Labsystem, Finland) at 485 (excitation) and 527 nm (emission). Antimycin (3 μ M, Sigma Chemical Co.), a potent inhibitor of Complex III in the electron transport chain, was used as a positive control.

Mitochondrial membrane potential ($\Delta\Psi_m$)

The $\Delta\Psi_m$ was assayed using the Mito-ID[®] Membrane Potential Kit according to the manufacturer's instructions (Enzo Life Sciences, Farmingdale, NY). Briefly, MCF-7 cells (8×10^3 per well) were seeded in 96-well plates. After 24 h, the cells were washed with PBS and loaded with Mito-ID Detection Reagent for 30 min at 37 °C in the dark. Afterwards, cells were washed with PBS and incubated with increasing concentrations of the tested complex. The fluorescence was estimated using a plate reader (Fluoroskan Ascent FL, Labsystem, Finland) at 490 (excitation) and 590 nm (emission).

Cellular thiols

MCF-7 cells (5×10^5) were seeded in 6-well plates in growth medium (4 mL). After 24 h, the cells were incubated for 24 and 48 h with increasing concentrations of the tested complex. Subsequently, the thiol content was measured as previously described.⁷

Total and oxidized intracellular glutathione

MCF-7 cells (3.5×10^5) were seeded in 6-well microplates in growth medium (4 mL). Following 48 h exposure to the tested complex at increasing concentrations, the cells were washed twice with PBS, treated with 6 % metaphosphoric acid and scraped. Samples were centrifuged and the supernatants were neutralized with Na₃PO₄ and assayed for total and oxidized glutathione following the procedure reported by Bindoli *et al.*⁸ Aliquots of pellets were dissolved in RIPA buffer and the protein content was determined.

Transmission electron microscopy

About 10^6 MCF-7 cells were seeded in 10 cm petri dishes. After 24 h the medium was removed and replaced with a fresh one containing the tested compound at the appropriate concentration. Subsequently, the cells were washed in cold PBS, harvested and directly fixed in 1.5 % glutaraldehyde buffered with 0.2 M sodium cacodylate, pH 7.4. After washing in the buffer and postfixation in 1 % OsO₄ in 0.2 M cacodylate buffer, specimens were dehydrated and embedded in epoxy resin (Epon Araldite). Sagittal serial sections (1 μ m) were counterstained with toluidine blue. Thin sections (90 nm) were given a contrast by staining with uranyl acetate and lead citrate.

Micrographs were taken with a Hitachi H-600 electron microscope (Hitachi, Tokyo, Japan) operating at 75 kV. All photos were typeset in Corel Draw 11.

***In vivo* anticancer activity toward Lewis Lung Carcinoma (LLC)**

All studies involving animal testing were carried out in accordance with the ethical guidelines for animal research adopted by the University of Padua, acknowledging the Italian regulation and European Directive 2010/63/UE as to the animal welfare and protection and the related codes of practice. The mice were purchased from Charles River, Italy, housed in steel cages under controlled environmental conditions (constant temperature, humidity, and 12 h dark/light cycle), and alimented with commercial standard feed and tap water ad libitum. The LLC cell line was purchased from ECACC, United Kingdom. The LLC cell line was maintained in DMEM (Euroclone) supplemented with 10 % heat inactivated fetal bovine serum (Euroclone), 10 mM L-glutamine, 100 units mL⁻¹ penicillin and 100 µg mL⁻¹ streptomycin in a 5 % CO₂ air incubator at 37 °C. The LLC was implanted intramuscularly (i.m.) as a 2 x 10⁶ cell inoculum into the right hind leg of 8 week old male and female C57BL mice (24 ± 3 g body weight). After 7 days from tumor implantation (visible tumor), the mice were randomly divided into 4 groups (5 animals per group) and subjected to daily i.p. administration of complex **1** (20 and 10 mg kg⁻¹ dissolved in a vehicle solution composed of 0.5 % DMSO (v/v) and 99.5 % of saline solution (v/v)), cisplatin (1.5 mg kg⁻¹ in saline solution), or the vehicle solution (0.5 % DMSO (v/v) and 99.5% of saline solution (v/v)). At day 15, the animals were sacrificed, the legs were amputated at the proximal end of the femur, and the inhibition of tumor growth was determined according to the difference in weight of the tumor-bearing leg and the healthy leg of the animals expressed as a percentage referring to the control animals. Body weight was measured every 2 days and was taken as a parameter for systemic toxicity. All reported values are the means ± SD of no less than three measurements.

Statistical analysis

All of the values are the means ± SD of not less than three measurements starting from three different cell cultures. Multiple comparisons were made by ANOVA followed by the Tukey–Kramer multiple comparison test (***P < 0.001; **P < 0.01; *P < 0.05), using GraphPad Software.

Computational methods

The 3D structure of the mTSPO-PK11195 complex as resolved in ref. 9 was obtained from the Protein Data Bank (accession code 2mgy). To identify a single structure from the NMR ensembles, we selected the structure in the ensemble that was closest to the average by RMSD. The Dock Prep module in Chimera¹⁰ was used for the assignment of the partial charges (according to AMBER parm99¹¹ force field) and to obtain the Mol2 file of the receptor. The molecular surface of the TSPO target was generated¹² (grey trace in Fig. S8) and the active site was identified by means of a set of overlapping spheres (cyan in Fig. S8) that creates the negative image of the surface invagination of the target in correspondence of the PK11195 binding site.

The geometries of the ligand PK11195, of the complex [CuBr₂(TZ6)] and of the precursors TZ6 and CuBr₂ have been first optimized in vacuum at the DFT level (cam-b3lyp functional, with Lanl2dz¹³⁻¹⁵ pseudopotential and basis set for the Cu atom and 6-31G(d,p) basis set for the ligand atoms). Partial atomic charges were calculated with the Restrained Electrostatic Potential (RESP) method¹⁶ which consists of fitting atomic charges to the molecular electrostatic potential generated at the HF/6-31G* level. Quantum calculations were performed with the program package Gaussian 09.¹⁷

For the rigid docking the scoring function is composed of intermolecular van der Waals (VDW) and electrostatic components. Since the receptor is considered to be rigid, the receptor contribution to the potential energy was pre-calculated and stored on a grid (of spacing 0.3 Å) according to the procedure implemented in DOCK 6.7.¹⁸ The search of the best pose is based on the anchor-and-grow algorithm, a breadth-first method for small molecule conformational sampling that involves placing rigid components in the binding site, followed by iterative segment growing and energy minimization. We searched a maximum of 1000 ligand orientations and allowed 500 iteration in the anchor-and-grow algorithm. The best poses obtained for PK11195, TZ6 and three poses of the complex [CuBr₂(TZ6)] are shown in Fig. S9, the corresponding values of the grid scoring function are reported in Table S5. The affinities evaluated by rigid docking of PK11195 and TZ6 for the target protein are comparable, while the interaction of 1 with the rigid binding pocket is repulsive because of the increased van der Waals radius due to the presence of the CuBr₂ moiety.

The AMBER Score implements molecular mechanics GB/SA simulations with the traditional all-atom AMBER force fields and the generalized AMBER force field.^{19,20} Topology files for the receptor and the two ligands TZ6 and [CuBr₂(TZ6)] were prepared within *xleap*.²¹ Missing parameters were assigned either by analogy with other atom types already defined in the force field or based on quantum mechanical calculations. In particular, the potential for the dihedrals involving the metal center Br-Cu-N-C and N-Cu-N-C angles were obtained by fitting quantum mechanical energies obtained by means of a relaxed PES (Potential Energy Surface) scan as shown in Fig. S10. The RESP partial atomic charges and GAFF atom types of the two ligand residues are given in Table S6.

We implemented the minimization/MD/minimization protocol²² consisting of 100 steps of minimization with a conjugate gradient method, followed by 3000 steps of molecular dynamics simulation at a constant temperature of 300 K by means of a Langevin thermostat,²³ another 100 steps of minimization, and a final energy evaluation. All atoms were allowed to move during the procedure. Fig. S11 reports the relaxed structures of poses a) and b) of the complex [CuBr₂(TZ6)].

Table S1 Crystallographic data for [CuBr₂(TZ6)] (**1**)

Formula	C ₁₈ H ₂₀ Br ₂ Cl ₂ CuN ₄ O ₅
<i>M_r</i>	634.70
Crystal color and habit	red parallelepiped
Crystal size	0.20 x 0.17 x 0.02
Crystal system	monoclinic
Space group	P2 ₁ /c
Unit cell dimensions	
<i>a</i> [Å]	14.226(2)
<i>b</i> [Å]	12.762(2)
<i>c</i> [Å]	13.867(1)
<i>β</i> [°]	117.14(1)
<i>V</i> [Å ³]	2240.4(5)
<i>Z</i>	4
<i>D</i> _{calc} (g cm ⁻³)	1.882
<i>μ</i> (Mo K _α) (mm ⁻¹)	4.892
<i>F</i> (000)	1252
2 θ range (°)	5.9 - 58.7
No. unique reflections (<i>R</i> _{int})	5707
No. of observed reflections	2126 (<i>I</i> > 2 σ (<i>I</i>))
No. of parameters	181
Final <i>R</i> ₁ , <i>wR</i> ₂	<i>R</i> ₁ = 8.6%, <i>wR</i> ₂ = 17.7%
(observed reflections) ^a	
Goodness-of-fit	1.020
(observed reflections)	

^a $R_1 = \sum ||F_o| - |F_c|| / \sum |F_o|$; $wR_2 = [\sum w(F_o^2 - F_c^2)^2 / \sum w(F_o^2)^2]^{1/2}$; $w^{-1} = \sigma^2(F_o^2) + (aP)^2$; $P = (F_o^2 + 2F_c^2)/3$.

Table S2 Experimental and optimized bond length (Å), angles (°) and torsion angles (°) in [CuBr₂(TZ6)] (**1**)

	experimental (e.s.d.)	optimized ^a
Cu1–N1	2.017(9)	2.1615
Cu1–N2	1.994(8)	2.1193
Cu1–Br1	2.322(2)	2.3235
Cu1–Br2	2.362(2)	2.3479
N1–Cu1–N2	80.9(4)	76.74
N1–Cu1–Br1	98.2(2)	98.18
N1–Cu1–Br2	131.0(3)	130.93
N2–Cu1–Br1	151.3(3)	150.15
N2–Cu1–Br2	98.9(3)	100.44
Br1–Cu1–Br2	102.95(7)	104.64
N1–C3–C4–N2	5.0(17)	5.46
C3–N1–Cu–Br1	-165.5(8)	-165.50
C4–N2–Cu–Br1	107.4(9)	107.44

^a optimized geometry in vacuum at DFT level (cam-b3lyp functional, with Lanl2dz pseudopotential and basis set for the Cu atom and 6-31G(d,p) basis set for all the other atoms as implemented in G09.

Table S3 Cells ($3\text{-}5 \times 10^4 \text{ mL}^{-1}$) were treated for 72 h with increasing concentrations of the tested compounds. The cytotoxicity was assessed by the MTT test. IC₅₀ values were calculated by a four parameter logistic model ($P < 0.05$). SD = standard deviation. RF = IC₅₀ resistant cells/IC₅₀ sensitive cells.

	IC ₅₀ (μM) ± SD		
	2008	C13*	RF
1	0.33 ± 0.07	0.23 ± 0.01	0.7
CDDP	2.17 ± 1.37	22.26 ± 1.86	10
	IC ₅₀ (μM) ± SD		
	LoVo	VoVo-OXP	RF
1	0.33 ± 0.07	0.23 ± 0.01	0.7
OXP	0.96 ± 0.51	16.44 ± 3.13	17
	IC ₅₀ (μM) ± SD		
	LoVo	LoVo MDR	RF
1	0.33 ± 0.07	0.46 ± 0.09	1
Doxorubicin	1.11 ± 0.51	19.36 ± 2.21	17

Table S4 Cells ($5 \times 10^4 \text{ mL}^{-1}$) were treated for 72 h with increasing concentrations of the tested compounds. The cytotoxicity was assessed by MTT test. IC_{50} values were calculated by 4-PL ($P < 0.05$).

	$\text{IC}_{50} (\mu\text{M}) \pm \text{SD}$		
	MRC-5	CCD18-Co	HEK293
1	19.59 ± 1.76	52.29 ± 3.74	20.87 ± 2.13
CDDP	19.23 ± 1.35	28.30 ± 1.53	19.56 ± 3.47
OXF	23.13 ± 1.25	27.14 ± 2.17	25.54 ± 1.65

Table S5 Values of the scoring functions (kcal/mol) for Rigid Docking and AMBER Score.^a For the Rigid Docking (RD) the van der Waals (vdW) and the electrostatic (es) contributions are reported.^a

	PK11195	TZ6	1 (a)	1 (b)	1 (c)
RD score:	-49.3	-52.6	15.3	29.7	436.7
vdW	-48.8	-50.1	16.5	25.9	437.2
es	-0.5	-2.5	-1.2	3.8	-0.5
Amber score	-	-51.7	-24.2	-29.3	-34.2

^a This method calculates the energy terms by employing an all atom force field,^[24-26] including bond, angle, and dihedral terms, as well as Coulomb interactions and the Lennard-Jones potential for the ligand, receptor and complex. The solvation energy is calculated using a Generalized Born solvation model.^[31] The structures of both the ligand and the TSPO receptor are allowed to change to maximize binding according to a minimization/molecular dynamics/minimization protocol (see section on computational methods).^[22]

Table S6 GAFF atom types and RESP partial atomic charges for TZ6 and [CuBr₂(TZ6)] (1)

TZ6				[CuBr ₂ (TZ6)]			
		Atom Type	RESP charges			Atom Type	RESP charges
				1	Cu	Cu	0.455921
				2	Br	br	-0.498614
				3	Br	br	-0.498614
1	Cl	cl	-0.0424	4	Cl	cl	0.038828
2	Cl1	cl	-0.0896	5	Cl1	cl	-0.070723
3	S	ss	-0.0171	6	S	ss	0.091642
4	N	nc	-0.4533	7	N	nc	0.008154
5	N1	nd	-0.6178	8	N1	nd	-0.366252
6	O	o	-0.5278	9	O	o	-0.534821
7	N2	na	0.0073	10	N2	na	0.030737
8	N3	n	-0.3114	11	N3	n	-0.249094
9	C	cc	0.0783	12	C	cc	-0.148605
10	H	h4	0.1405	13	H	h4	0.205582
11	C1	cd	-0.3445	14	C1	cd	-0.250774
12	H1	h4	0.234	15	H1	h4	0.247651
13	C2	cd	0.4668	16	C2	cd	0.128939
14	C3	cd	0.0834	17	C3	cd	0.001826
15	C4	cc	-0.1438	18	C4	cc	-0.085992
16	C5	c2	-0.0916	19	C5	c2	-0.050207
17	H2	h4	0.1971	20	H2	h4	0.17293
18	C6	c2	-0.07	21	C6	c2	-0.043011
19	C7	c2	0.0308	22	C7	c2	0.065233
20	H3	ha	0.1434	23	H3	ha	0.144404
21	C8	c2	-0.2318	24	C8	c2	-0.255212
22	C9	cc	0.6272	25	C9	cc	0.510944
23	C10	c3	-0.0117	26	C10	c3	0.099504
24	H4	hc	0.045	27	H4	hc	0.008649
25	H5	hc	0.045	28	H5	hc	0.008649
26	C11	c	0.5226	29	C11	c	0.525864
27	C12	c3	0.0382	30	C12	c3	-0.00678
28	H6	h1	0.0376	31	H6	h1	0.047357
29	H7	h1	0.0376	32	H7	h1	0.047357
30	C13	c3	0.0734	33	C13	c3	0.064528
31	H8	hc	0.004	34	H8	hc	0.014383
32	H9	hc	0.004	35	H9	hc	0.014383
33	C14	c3	-0.1071	36	C14	c3	-0.128834
34	H10	hc	0.026	37	H10	hc	0.033612
35	H11	hc	0.026	38	H11	hc	0.033612
36	H12	hc	0.026	39	H12	hc	0.033612
37	C15	c3	0.0382	40	C15	c3	-0.00678

38	H13	h1	0.0376	41	H13	h1	0.047357
39	H14	h1	0.0376	42	H14	h1	0.047357
40	C16	c3	0.0734	43	C16	c3	0.064528
41	H15	hc	0.004	44	H15	hc	0.014383
42	H16	hc	0.004	45	H16	hc	0.014383
43	C17	c3	-0.1071	46	C17	c3	-0.128834
44	H17	hc	0.026	47	H17	hc	0.033612
45	H18	hc	0.026	48	H18	hc	0.033612
46	H19	hc	0.026	49	H19	hc	0.033612

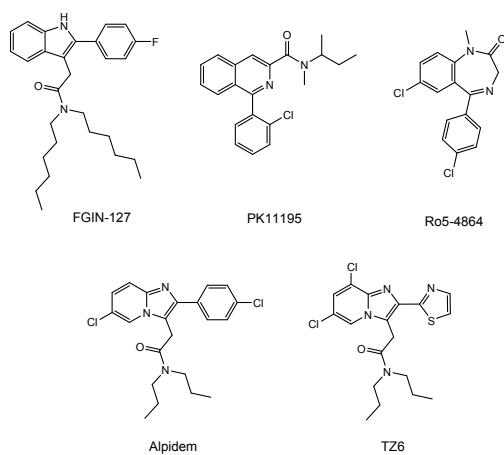


Fig. S1 Examples for TSPO ligands reported in the literature.^[28-31]

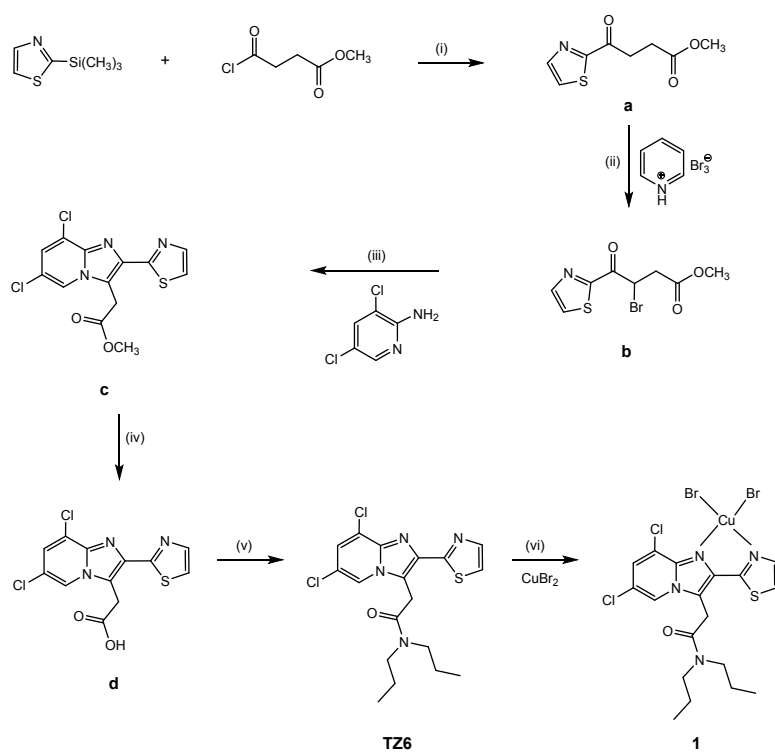


Fig. S2 Synthesis of $[\text{CuBr}_2(\text{TZ6})]$ (**1**): (i) 0 °C; (ii) THF, 50 °C; (iii) EtOH, 90 °C; (iv) BuOH / 0.4 M NaOH; (v) 6-Cl-HOBT / N,N' -diisopropylcarbodiimide / THF; (vi) CH_3CN / CH_2Cl_2 .

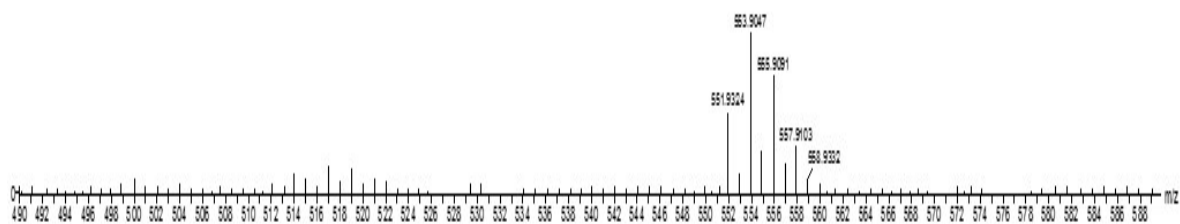
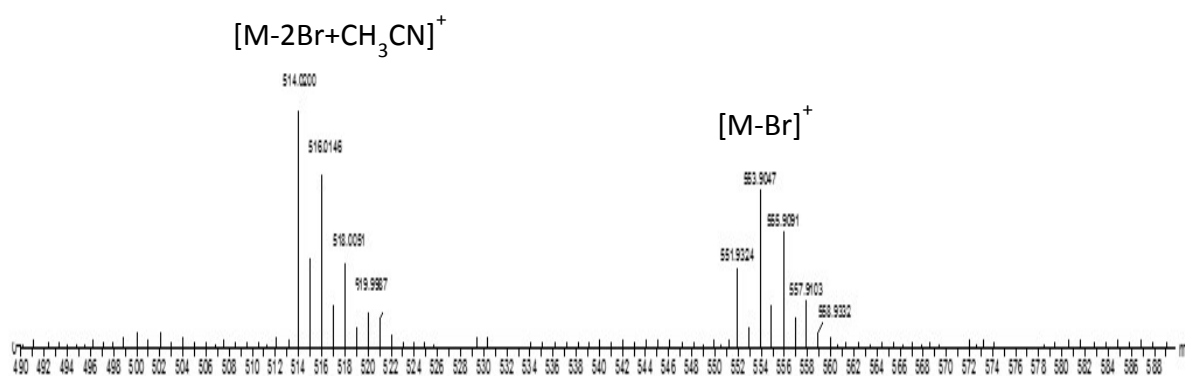
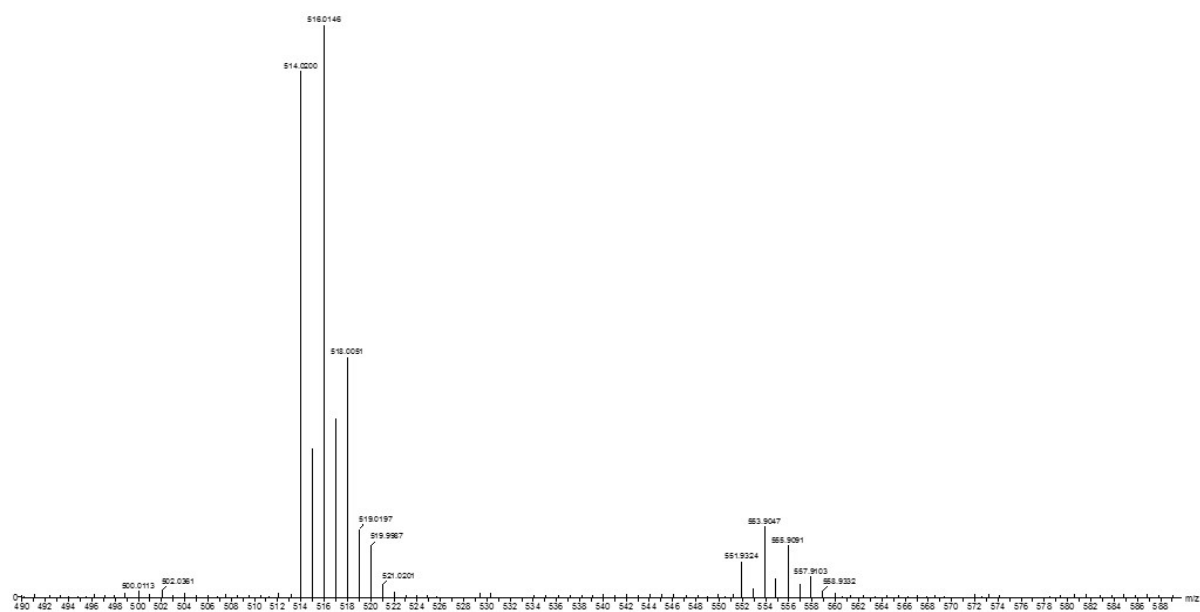
A**B****C**

Fig. S3 ESI-MS spectra of **1** dissolved in 0.9 % NaCl solution containing 0.1 % CH₃CN. A) fresh solution; B) after 48 h; C) after 1 week.

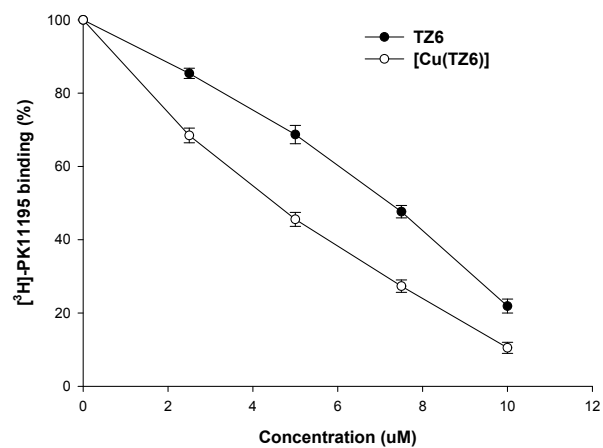


Fig. S4 [³H]PK11195 TSPO binding competition studies. Displacement of [³H]PK11195 by TZ6 and [CuBr₂(TZ6)] in crude mitochondrial membrane homogenates obtained from MCF-7 cells. Samples were incubated with 3 nM of [³H]PK11195 in the presence of increasing concentrations of TZ6 and [Cu Br₂(TZ6)]. Results are presented as mean ± SD of three separate experiments.

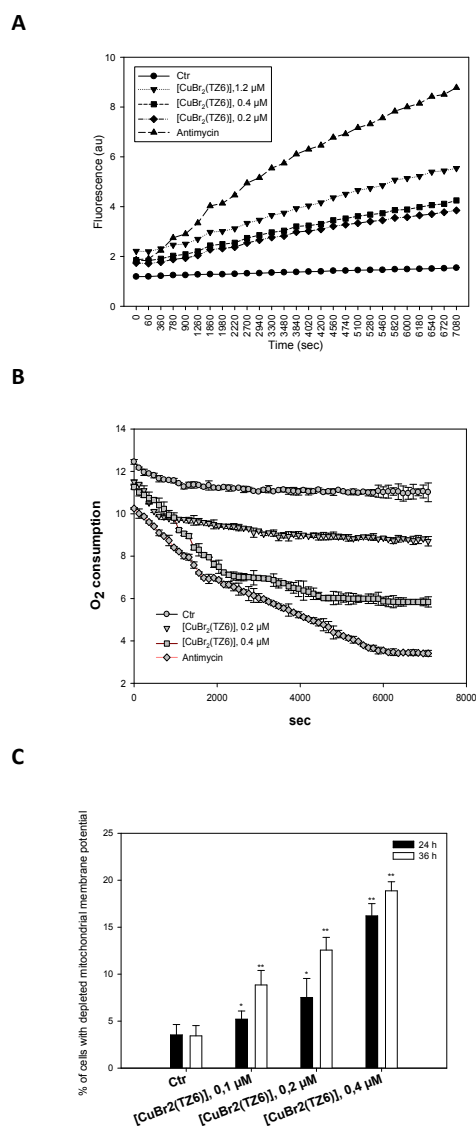


Fig. S5 Effects of **1** on the mitochondria. **A.** ROS production in MCF-7 cells. Cells were pre-incubated in PBS/10 mM glucose medium for 20 min at 37 °C in the presence of 10 mM CM-H₂DCFDA and then treated with increasing concentrations of **1** or antimycin (3 μM). The fluorescence of DCF was measured at 485 nm (excitation) and 527 nm (emission). **B.** Effects of **1** on O₂ consumption. MCF-7 cells were treated with Mito-ID® O₂ Sensor Probe Solution containing IC₅₀ doses of the tested compound. The fluorescence was estimated at 350 nm (excitation) and 610 nm (emission). Error bars indicate SD. **C.** Effects of **1** on the mitochondrial membrane potential. MCF-7 cells were treated for 24 or 36 h with increasing concentrations of **1** or antimycin (3 μM) and stained with TMRM (10 nM). The fluorescence was estimated at 490 nm (excitation) and 590 nm (emission). Error bars indicate SD. * p < 0.05; ** p < 0.01.

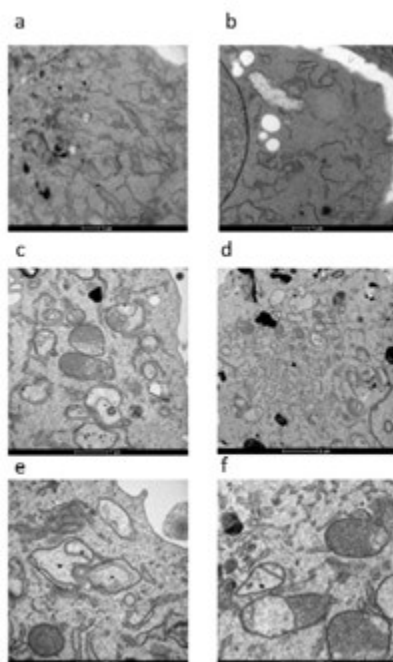


Fig. S6 TEM analysis of MCF-7 cells treated for 12 or 24 h with **1** at IC_{50} concentration. Cells were processed through standard procedures as described above. a) and b) Control; c) and d) **1**, 12 h; e) and f) **1**, 24 h.

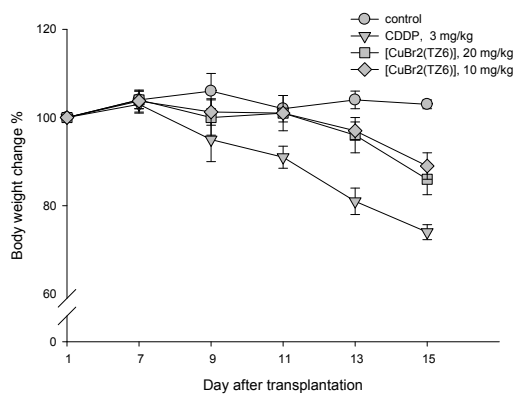


Fig. S7 Body weight changes of LLC bearing C57BL mice treated with vehicle or tested compounds. Each drug was administered daily after 7 days from the tumor cell inoculum. Weights were measured at day 1 and daily from day 7. Error bars indicate SD.

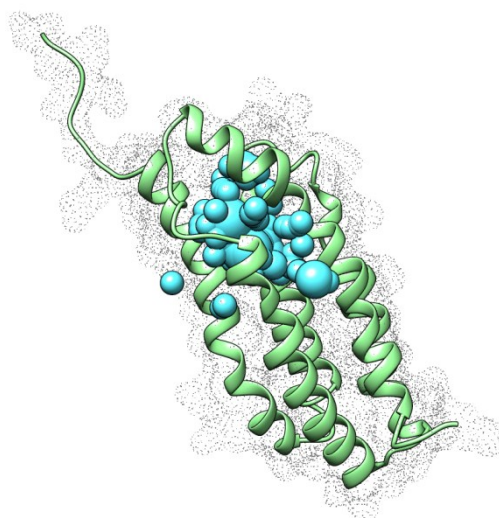


Fig. S8 Molecular surface and identification of the binding pocket in the TSPO target.

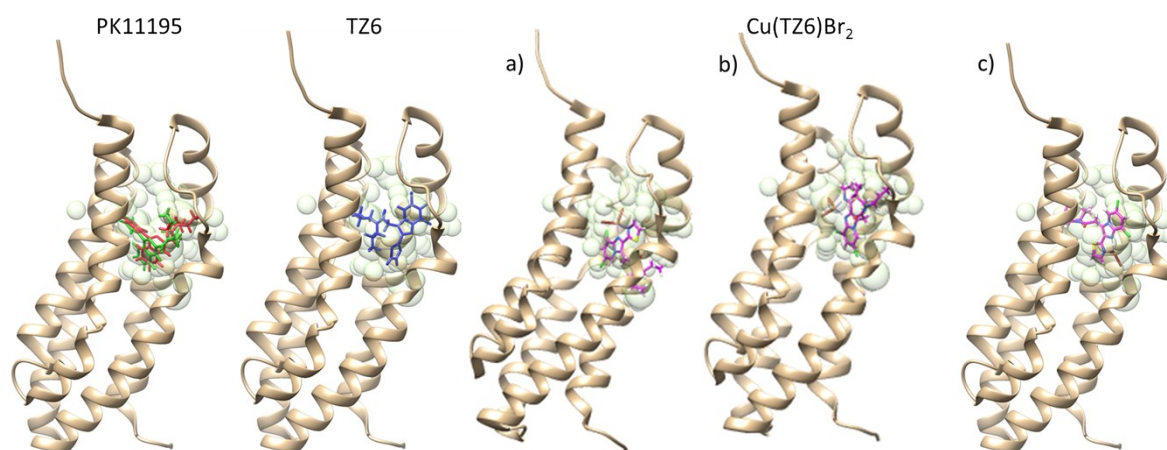


Fig. S9 Poses of the ligands obtained with the rigid docking protocol. The best pose of PK11195 (red) is superimposed to the crystallographic pose (green). For the complex CuBr₂(TZ6) the three poses a), b) and c) that were subsequently used as starting structures for the Amber Score procedure are shown.

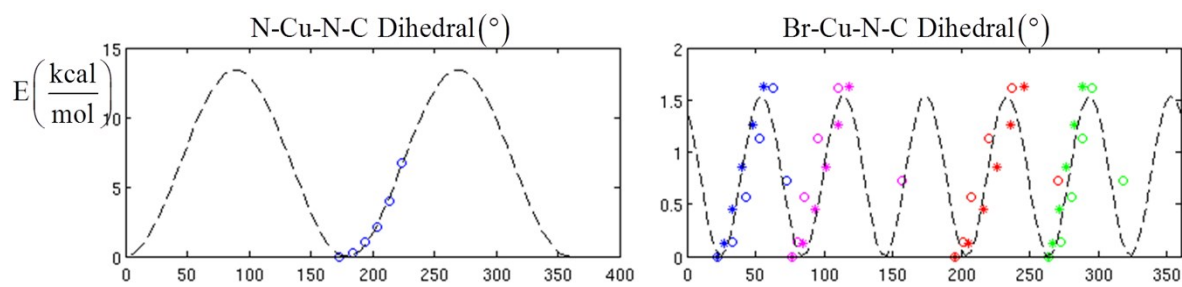


Fig. S10 Energies obtained from relaxed PES scan computations (cam-b3lyp/ Lanl2dz/ 6-31G(d,p)) and relative fitting (dashed line) with the standard function $PK/IDIVF (1 + \cos(PN \phi - PHASE))$.

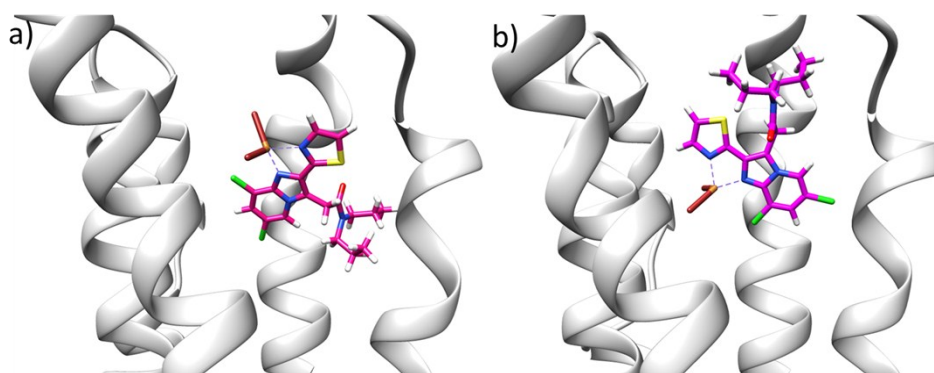


Fig. S11 Structures a) and b) of the TSPO- $\text{CuBr}_2(\text{TZ6})$ complex after the the minimization/MD/ minimization protocol.

References

- 1 N. Margiotta, R. Ostuni, R. Ranaldo, N. Denora, V. Laquintana, G. Trapani, G. Liso and G. Natile, *J. Med. Chem.*, 2007, **50**, 1019–1027.
- 2 CrysAlisPro, Oxford Diffraction Ltd., Version 1.171.33.31 (release 08-01-2009 CrysAlis171.NET).
- 3 (a) SHELXT – G. M. Sheldrick, *Acta Crystallogr.*, 2015, **A71**, 3–8. (b) SHELXL - G. M. Sheldrick, *Acta Crystallogr.*, 2015, **C71**, 3-8.
- 4 P. McArdle, K. Gilligan, D. Cunningham, R. Dark and M. Mahon, *CrystEngComm.*, 2004, **6**, 303-309.
- 5 P. McArdle, PC Windows version, *J. Appl. Cryst.*, 1995, **28**, 65-65.
- 6 N. Margiotta, S. Savino, C. Marzano, C. Pacifico, J. D. Hoeschele, V. Gandin and G. Natile, *J. Inorg. Biochem.*, 2016, **160**, 85-93.
- 7 M. Pellei, V. Gandin, M. Marinelli, A. Orsetti, F. Del Bello, C. Santini and C. Marzano, *Dalton Trans.*, 2015, **44**, 21041-21052.
- 8 A. Bindoli, M. T. Callegaro, E. Barzon, M. Benetti and M. P. Rigobello, *Arch. Biochem. Biophys.*, 1997, **342**, 22-28.
- 9 L. Jaremko, M. Jaremko, K. Giller, S. Becker and M. Zweckstetter, *Science*, 2014, **343**, 1363-1366.
- 10 E. F. Pettersen, T. D. Goddard, C. C. Huang, G. S. Couch, D. M. Greenblatt, E. C. Meng and T. E. Ferrin, *J. Comput. Chem.*, 2004, **25**, 1605-1612.
- 11 W. D. Cornell, P. Cieplak, C. I. Bayly, I. R. Gould, K. M. Merz, D. M. Ferguson, D. C. Spellmeyer, T. Fox, J. W. Caldwell and P. A. Kollman, *J. Am. Chem. Soc.*, 1995, **117**, 5179-5197.
- 12 F. M. Richards, *Annu. Rev. Biophys. Bioeng.*, 1977, **6**, 151-176.
- 13 P. J. Hay and W. R. Wadt, *J. Chem. Phys.*, 1985, **82**, 270-283.
- 14 P. J. Hay and W. R. Wadt, *J. Chem. Phys.*, 1985, **82**, 299-310.
- 15 W. R. Wadt and P. J. Hay, *J. Chem. Phys.* 1985, **82**, 284-298.
- 16 C. I. Bayly, P. Cieplak, W. Cornell and P. A. Kollman, *J. Phys. Chem.*, 1993, **97**, 10269-10280.
- 17 Gaussian 09, Revision A.02, M. J. Frisch, G. W. Trucks, H. B. Schlegel, G. E. Scuseria, M. A. Robb, J. R. Cheeseman, G. Scalmani, V. Barone, B. Mennucci, G. A. Petersson, H. Nakatsuji, M. Caricato, X. Li, H. P. Hratchian, A. F. Izmaylov, J. Bloino, G. Zheng, J. L. Sonnenberg, M. Hada, M. Ehara, K. Toyota, R. Fukuda, J. Hasegawa, M. Ishida, T. Nakajima, Y. Honda, O. Kitao, H. Nakai, T. Vreven, J. A. Montgomery, Jr., J. E. Peralta, F. Ogliaro, M. Bearpark, J. J. Heyd, E. Brothers, K. N. Kudin, V. N. Staroverov, R. Kobayashi, J. Normand, K. Raghavachari, A. Rendell, J. C. Burant, S. S. Iyengar, J. Tomasi, M. Cossi, N. Rega, J. M. Millam, M. Klene, J. E. Knox, J. B. Cross, V. Bakken, C. Adamo, J. Jaramillo, R. Gomperts, R. E. Stratmann, O. Yazyev, A. J. Austin, R. Cammi, C. Pomelli, J. W. Ochterski, R. L. Martin, K. Morokuma, V. G. Zakrzewski, G. A. Voth, P. Salvador, J. J. Dannenberg, S. Dapprich, A. D. Daniels, Ö. Farkas, J. B. Foresman, J. V. Ortiz, J. Cioslowski and D. J. Fox, *Gaussian, Inc., Wallingford CT*, 2009.
- 18 P. T. Lang, S. R. Brozell, S. Mukherjee, E. F. Pettersen, E. C. Meng, V. Thomas, R. C. Rizzo, D. A. Case, T. L. James and I. D. Kuntz, *RNA*, 2009, **15**, 1219-1230.
- 19 D. A. Case, T. E. Cheatham, T. O. M. Darden, H. Gohlke, R. A. Y. Luo, K. M. Merz, A. Onufriev, C. Simmerling, B. Wang and R. J. Woods, *J. Comput. Chem.*, 2005, **26**, 1668-1688.
- 20 J. Wang, R. M. Wolf, J. W. Caldwell, P. A. Kollman and D. A. Case, *J. Comput. Chem.*, 2004, **25**, 1157-1174.
- 21 Case, D. A., T. A. Darden, T. E. Cheatham, C. L. Simmerling, J. Wang, R. E. Duke, R. Luo, R. C. Walker, W. Zhang, K. M. Merz, B. Roberts, S. Hayik, A. Roitberg, G. Seabra, J. Swails, A. W.

- Goetz, I. Kolossváry, K. F. Wong, F. Paesani, J. Vanicek, R. M. Wolf, J. Liu, X. Wu, S. R. Brozell, T. Steinbrecher, H. Gohlke, Q. Cai, X. Ye, J. Wang, M. J. Hsieh, G. Cui, D. R. Roe, D. H. Mathews, M. G. Seetin, R. Salomon-Ferrer, C. Sagui, V. Babin, T. Luchko, S. Gusarov, A. Kovalenko and P. A. Kollman, *AMBER 12*, University of California, San Francisco, 2012.
- 22 A. P. Graves, D. M. Shivakumar, S. E. Boyce, M. P. Jacobson, D. A. Case and B. K. Shoichet, *J. Mol. Biol.* 2008, **377**, 914-934.
- 23 M. P. Allen and D. J. Tildesley, *Computer Simulation of Liquids*, Clarendon Press, 1989.
- 24 W. D. Cornell, P. Cieplak, C. I. Bayly, I. R. Gould, K. M. Merz, D. M. Ferguson, D. C. Spellmeyer, T. Fox, J. W. Caldwell and P. A. Kollman, *J. Am. Chem. Soc.*, 1995, **117**, 5179–5197.
- 25 A. Pérez, I. Marchan, D. Svozil, J. Sponer, T. E. Cheatham, C. A. Lughton and M. Orozco, *Biophys. J.*, 2007, **92**, 3817–3829.
- 26 J. Wang, R. M. Wolf, J. W. Caldwell, P. A. Kollman and D. A. Case, *J. Comput. Chem.*, 2004, **25**, 1157–1174.
- 27 A. Onufriev, D. Bashford and D. A. Case, *Proteins: Struct., Funct., Bioinf.*, 2004, **55**, 383–394.
- 28 E. Romeo, J. Auta, A. P. Kozikowski, D. Ma, V. Papadopoulos, G. Puia, E. Costa and A. Guidotti, *J. Pharmacol. Exp. Ther.*, 1992, **262**, 971-978.
- 29 G. Le Fur, M. L. Perrier, N. Vaucher, F. Imbault, A. Flamier, J. Benavides, A. Uzan, C. Renault, M. C. Dubroeuq and C. Gueremy, *Life Sci.*, 1983, **32**, 1839-1847.
- 30 P. J. Marangos, J. Patel, J. P. Boulenger and R. Clark-Rosenberg, *Mol. Pharmacol.*, 1982, **22**, 26-32.
- 31 S. Z. Langer, S. Arbilla, S. Tan, K. G. Lloyd, P. George, J. Allen and A. E. Wick, *Pharmacopsychiatry*, 1990, **23**, 103-107.